



HAL
open science

Tuning the properties of porous chitosan: Aerogels and cryogels

Coraline Chartier, Sytze Buwalda, H el ene van den Berghe, Benjamin Nottelet,
Tatiana Budtova

► **To cite this version:**

Coraline Chartier, Sytze Buwalda, H el ene van den Berghe, Benjamin Nottelet, Tatiana Budtova. Tuning the properties of porous chitosan: Aerogels and cryogels. *International Journal of Biological Macromolecules*, 2022, 202, pp.215-223. 10.1016/j.ijbiomac.2022.01.042 . hal-03576736

HAL Id: hal-03576736

<https://hal.science/hal-03576736v1>

Submitted on 27 Feb 2023

HAL is a multi-disciplinary open access archive for the deposit and dissemination of scientific research documents, whether they are published or not. The documents may come from teaching and research institutions in France or abroad, or from public or private research centers.

L'archive ouverte pluridisciplinaire **HAL**, est destin ee au d ep ot et  a la diffusion de documents scientifiques de niveau recherche, publi es ou non,  emanant des  tablissements d'enseignement et de recherche franais ou  trangers, des laboratoires publics ou priv es.

Submitted to the International Journal of Biological Macromolecules 26 October 2021

Revised version submitted 26 December 2021

Tuning the properties of porous chitosan: aerogels and cryogels

*Coraline Chartier,^a Sytze Buwalda,^a H  l  ne Van Den Berghe,^b Benjamin Nottelet,^b
Tatiana Budtova^{a*}*

^a MINES ParisTech, PSL Research University, Center for Materials Forming (CEMEF), UMR
CNRS 7635, CS 10207, 06904 Sophia Antipolis, France

^b Department of Polymers for Health and Biomaterials, IBMM, Univ Montpellier, CNRS, ENSCM,
Montpellier, France.

*Corresponding author: Tatiana Budtova, tatiana.budtova@minesparis.psl.fr

Highlights

- Chitosan aerogels and cryogels were prepared *via* supercritical CO₂ drying and freeze-drying, respectively
- The influence of process parameters on materials' structure and properties was studied
- Aerogels possessed a higher density and higher specific surface area than cryogels
- The absorption of simulated wound exudate was investigated

Abstract

Highly porous chitosan-based materials were prepared via dissolution, non-solvent induced phase separation and drying using different methods. The goal was to tune the morphology and properties of chitosan porous materials by varying process parameters. Chitosan concentration, concentration of sodium hydroxide in the coagulation bath and aging time were varied. Drying was performed *via* freeze-drying leading to “cryogels” or *via* drying with supercritical CO₂ leading to “aerogels”. Cryogels were of lower density than aerogels (0.03 - 0.12 g/cm³ vs 0.07 - 0.26 g/cm³, respectively) and had a lower specific surface area (50 – 70 vs 200 – 270 m²/g, respectively). The absorption of simulated wound exudate by chitosan aerogels and cryogels was studied in view of their potential applications as wound dressing. Higher absorption was obtained for cryogels (530 – 1500 %) as compared to aerogels (200 – 610 %).

Keywords: density; specific surface area; porosity, freeze-drying, supercritical drying

1. INTRODUCTION

A porous 3D biomaterial can be generated by removing the solvent from a “wet” polymer network. The properties of the porous material depend greatly on the drying method of the precursor [1,2]. Aerogels are obtained *via* drying under supercritical (sc) conditions, most often using sc CO₂. Since no liquid-vapor meniscus exists under sc conditions, capillary stresses, which usually lead to collapse of pore walls under ambient pressure drying, are no longer acting. The structure of the gel is therefore theoretically kept intact, leading to a nanostructured material with high porosity and high internal pores’ surface area. This is in contrast with freeze-drying (for simplicity we will call such materials cryogels), where the growth of ice crystals may distort the network structure and lead to the formation of larger pores and a lower internal surface area. Materials obtained *via* ambient pressure or vacuum drying, so-called xerogels, often have a high density and low porosity due to collapse of pore walls. Both aerogels and cryogels possess particular properties in terms of density, morphology, pore size distribution and surface area. The understanding of processing-structure-properties correlations is therefore essential for matching the requested application.

Chitosan is a semi-natural polymer which can be obtained *via* deacetylation of chitin which in turn is extracted from crustacean shells. It is a cationic polymer composed of D-glucosamine and N-acetyl-D-glucosamine linked by β (1 \rightarrow 4) glycosidic bonds. Thanks to its antiviral, antibacterial and antifungal properties as well as its biocompatibility, chitosan has been frequently used for biomedical applications, including wound dressings and drug delivery systems [3–5]. Several examples of porous chitosan-based biomaterials, including cryogels and aerogels, exist in literature, as reviewed recently [6,7]. For example, pH-responsive chitosan [8] and hybrid chitosan-cellulose-graphene oxide [9] cryogels were developed for drug delivery applications. Drug-loaded

chitosan aerogel particles prepared *via* the dropping [10] or jet cutting method [11] were suggested for wound healing applications.

In order to obtain chitosan aerogels or cryogels, various approaches exist. In all cases chitosan is first dissolved, usually in acidic medium. In order to form a network, chitosan can then be either crosslinked *via* its amino groups (using formaldehyde [12], urea [13], glutaraldehyde [14] or sodium tripolyphosphate [15]), or directly coagulated in a non-solvent (for example, in a basic solution). In the latter case non-solvent induced phase separation (or immersion precipitation) occurs: chitosan forms a network with non-solvent in the pores. To use drying with sc CO₂, the liquid in the pores of a network (crosslinked or not) must be miscible with CO₂, and thus solvent exchange step is often applied. Quignard et al. used the non-solvent induced phase separation method for the preparation of chitosan beads in NaOH-water; NaOH was then removed by washing the beads in water followed by exchange of water to ethanol and sc CO₂ drying, resulting in chitosan aerogel beads [16]. The same approach was used in refs. [10] and [11]. Chemical crosslinking is supposed to lead to better mechanical properties and a more homogeneous network structure [14], but the use of toxic crosslinkers (e.g. glutaraldehyde) may lead to adverse effects in biomedical applications.

In the vast majority of publications only one method of drying is used for the preparation of the chitosan porous material, which impedes the in-depth understanding of processing-structure-properties correlations of chitosan porous materials. To the best of our knowledge, only two articles compare the properties of sc dried and freeze-dried chitosan starting from the same precursor, and in both cases chitosan was crosslinked. Obaidat et al. prepared sc CO₂ and freeze-dried beads based on chitosan crosslinked with sodium tripolyphosphate [15]. The specific surface area of aerogels was 70 – 100 m²/g and for cryogels it was not detectable. Takeshita et al. made sc CO₂ and freeze-dried (from water and from tert-butanol) chitosan crosslinked with formaldehyde and reported

much a higher value for the specific surface area of aerogels, almost 500 m²/g. For the cryogel, as in the case above, the surface area was not detectable [17]. In the present work, for the first time, the influence of drying conditions (freeze-drying versus sc drying) on the structural and physico-chemical properties of non-crosslinked chitosan porous materials was investigated starting from the same chitosan precursor. We also analyzed the influence of chitosan and NaOH concentrations in the coagulation bath and of aging time. In the view of potential biomedical applications of these porous chitosan materials, the absorption of simulated wound exudate was evaluated.

2. EXPERIMENTAL

2.1. Materials

All chemicals were used as received. Chitosan of high molecular weight (600 – 800 kDa according to the manufacturer) was purchased from Acros; the exact molecular weight was determined with viscometry and is presented in the Results and Discussion section. The degree of acetylation was determined by infrared spectroscopy with the method described by Moore and Roberts [18] (see Methods section). Glacial acetic acid, ethanol (purity higher than 99 %) and sodium hydroxide pellets (analytical reagent grade) were supplied by Fisher Chemical. Water was distilled.

2.2. Methods

2.2.1. Preparation of chitosan cryogels and aerogels

Chitosan was dissolved in a solution of 2 % v/v acetic acid under mechanical stirring at room temperature for several hours. The concentration of chitosan was varied from 1 to 10 % wt/v. Around 6 mL of chitosan solution was poured into polypropylene molds of 27.5 mm in diameter with holes in the walls of 1 mm in diameter. The molds were immersed in 100 mL of aqueous

NaOH solution (0.1 – 4 M at various durations called “aging”) for non-solvent induced phase separation. As NaOH-water is chitosan non-solvent, the polymer coagulated, but most of the samples kept their 3D shape. The holes in the mold were made for non-solvent penetration from all sides of chitosan solution thus leading to homogeneous coagulation. NaOH was then washed out with water by placing the sample in consecutive water baths, resulting in a “hydrogel” (Fig. 1).

Figure 1

In order to obtain “aerogels”, drying was performed with sc CO₂ (Fig. 1). As water is not miscible with CO₂, water in the hydrogels was replaced by ethanol as follows. The chitosan hydrogels were gently demolded and immersed in mixtures of ethanol and distilled water. The ethanol fraction was gradually increased over the course of three days (10/90, 25/75, 50/50, 75/25, 90/10, 100/0) to remove water. To ensure a complete solvent exchange, several washing steps with pure ethanol were performed during two days. This solvent exchange resulted in chitosan “alcogels” (Fig. 1).

Drying with sc CO₂ was performed as described elsewhere [19,20]. The system was pressurized at 50 bar and 37 °C, and ethanol was slowly washed with gaseous CO₂. Afterwards, the pressure in the autoclave was increased to 80 bars to be above the CO₂ critical point. The sc CO₂ solubilized the residual non-solvent inside the sample pores. At 37°C, a dynamic washing step was performed with an output of 5 kg of CO₂/h for 1 h. It was followed by a static mode of 1 – 2 h in the same conditions and then a dynamic step for 2 h again. The system was then depressurized at 4 bar/h and cooled to room temperature before opening the autoclave.

To obtain “cryogels”, hydrogels were freeze-dried by first immersing in liquid nitrogen (-196 °C) for 5 min and then placing in a freeze-dryer (Cryotec Cosmos 80) for lyophilization for 48 h.

“Xerogel” was obtained from a hydrogel made from 5 % wt/v chitosan solution coagulated in 4 M NaOH, aged for 24 h and dried at 55°C under vacuum until the constant weight.

2.2.2. Characterization

Chitosan molecular weight was determined from the intrinsic viscosity using the Mark-Houwink equation using an aqueous solution containing 0.1 M of acetic acid and 0.2 M of NaCl at 25 °C [21]:

$$[\eta] = KM^\alpha \quad (1)$$

with $K = 1.81 \times 10^5$ dL/g and $\alpha = 0.93$ [21].

Chitosan degree of acetylation (DA) was determined by infrared spectroscopy with the method described by Moore and Roberts [18]. The chitosan powder (4 mg) and 100 mg of KBr were dried for 4 h at 80 °C and mechanically blended to make a disk. Then the degree of DA was determined with the equation:

$$DA(\%) = (A_{1655}/A_{3450}) \times (100/1.33) \quad (2)$$

with A_{1655} the absorption at 1655 cm^{-1} of the amide I band and A_{3450} the absorption at 3450 cm^{-1} of the hydroxyl groups.

The evolution of sample volume at each processing step (for aerogels: from solution to alcogel and from alcogel to aerogel; for cryogels: from solution to hydrogel and from hydrogel to cryogel) and total shrinkage (from solution to dry matter, see Fig. 1) was monitored. As samples were of cylindrical shape, their diameter and height were measured, and volume shrinkage was calculated according to the following equation:

$$\text{Shrinkage} (\%) = (V_i - V_f) \times 100 / V_i \quad (4)$$

where V_i and V_f are sample volumes before and after the step, respectively.

The bulk density ρ_{bulk} was measured with an Envelope Density Analyzer Geopyc 1360 (Micromeritics) with a calibrated chamber using DryFlo fine powder. Porosity was calculated from bulk and skeletal density (ρ_{skeletal} , $1.446 \pm 0.116 \text{ g/cm}^3$ for chitosan [10]) with equation (5).

$$\text{Porosity (\%)} = (\rho_{\text{skeletal}} - \rho_{\text{bulk}}) \times 100 / \rho_{\text{skeletal}} \quad (5)$$

Pore specific volume was estimated using bulk and skeletal densities:

$$V_{\text{pore}} = (1/\rho_{\text{bulk}}) - (1/\rho_{\text{skeletal}}) \quad (6)$$

The specific surface area was measured using a Micromeritics ASAP 2020 employing the Brunauer, Emmett et Teller (BET) method. Prior to measurement the samples were degassed in a high vacuum at $70 \text{ }^\circ\text{C}$ for 10 h.

The morphology of the samples was studied with a Scanning Electron Microscope MAIA (Tescan) equipped with a field emission gun at an accelerating voltage of 3 keV. A layer of platinum was coated (14 nm) using a Q150T Quorum rotating metallizer.

It is now accepted that it is not possible to obtain the complete pore size distribution in bio-aerogels using nitrogen adsorption (BJH method) or mercury porosimetry [19,22,23]. The BJH approach takes into account mesopores and small macropores thus providing only 10–15 % of the total pore volume, and mercury does not enter the pores but compresses the sample. The pore size distribution in chitosan aerogels and cryogels was therefore roughly estimated with the software Visilog from the SEM images; at least 270 pores per formulation were analyzed.

X-ray diffraction patterns were obtained on powder samples with a ‘XPRT-PRO’ diffractometer from PANalytical equipped with a θ/θ 3050/60 goniometer, a $\text{CuK}\alpha$ source operated at 40 kV and 30 mA, and the measurement program ‘ScanPixcel’. The diffraction angle 2θ was from 5° to 40° with a 0.08° step.

Dried samples were immersed in simulated wound exudate (SWE) composed of 8.3 g/L of NaCl and 0.37 g/L of CaCl₂ at 31 °C (no viscosity modifier was used in agreement with the norm EN 13726-1). The evolution of sample weight W_t in time was measured during 48 h, and SWE absorption was calculated with the following equation:

$$Absorption(\%) = ((W_t - W_i) \times 100) / W_i \quad (7)$$

where W_i is sample initial weight.

3. RESULTS AND DISCUSSION

The results are presented as follows. First, the determination of the molecular weight and degree of acetylation of chitosan will be shown. Then, each material property, namely volume shrinkage, density, porosity, morphology, specific surface area and absorption of SWE will be presented and discussed for aerogels and cryogels as a function of various parameters such as the chitosan concentration, the concentration of NaOH in the coagulation bath, the aging time and the method of drying.

3.1. Determination of chitosan molecular weight and degree of acetylation

The intrinsic viscosity of chitosan was determined as described in Methods [21] and found to be 4.87 dL/g. The molecular weight was estimated to be around 691000 g/mol, which is in the range of the molecular weight given by the manufacturer, 600 – 800 kg/mol.

The degree of acetylation was determined as described in the Methods section [18] and found to be 10 ± 2 %.

3.2. Visual appearance

Photos of chitosan aerogels and cryogels made under different conditions are presented in Fig. 2. Higher is the concentration of chitosan, more stable is the shape of the hydrogel (and of the corresponding aerogel or cryogel), as seen in Fig. 2. For example, for 1 % wt/v of dissolved chitosan coagulated in 4 M NaOH, a fluffy aerogel with no distinct shape was obtained, and no adequate characterization of this sample was possible. A minimum of 3 % wt/v chitosan is necessary for the sample to keep the shape of the mold upon coagulation; a similar result was observed for cellulose aerogels despite that the molecular weight of cellulose was much lower, around 30-35 kDa [2]. No influence on the aerogel shape of NaOH concentration in the coagulation bath above 1 M was observed. Below 1 M NaOH, the hydrogel was soft and weak and the corresponding aerogel as well.

Figure 2

The cryogels have a similar visual appearance as aerogels (Fig. 2), but cracks are visible along the samples. They were formed during freezing because of the growing ice crystals. At higher chitosan concentrations, the samples present less cracks and are harder.

Xerogel photo is shown in Fig. S1 of the Supporting Information. The xerogel is brownish and partly translucent, with distorted shape and cracks most probably because of the significant and heterogeneous shrinkage.

3.3. Shrinkage

Volume shrinkage at different steps of the process and total shrinkage (eq. 2) are presented in Fig. 3 for aerogels and cryogels as a function of the chitosan concentration in the initial solution (Fig. 3a), of the NaOH concentration in the coagulation bath (Fig. 3b) and of the aging time (Fig.

3c). Because of a significant total shrinkage of the xerogel, around 80 %, only one sample was prepared and analyzed. Data known from literature for non-crosslinked chitosan aerogels and cryogels are also shown in Table S1 for comparison.

During coagulation and solvent exchange, a small volume decrease within 20 % was observed (Fig. 3). Polymer chains are supposed to strongly contract when a solvent is replaced by a non-solvent; this is well known for synthetic polyelectrolyte polymer gels [24]. Interestingly, chitosan is not shrinking much, most probably because the non-solvent used is an aqueous medium which has a high affinity for chitosan, and also because of polysaccharide chain rigidity. Rather low shrinkage in a non-solvent was also observed for cellulose, pectin and high-amylose starch [2,20,25]. Shrinkage during *sc* CO₂ drying is similar to the one during coagulation and solvent exchange, leading to a total shrinkage around 30 - 40 % which does not depend on process parameters within the intervals studied and experimental errors. Neither polymer concentration (Fig. 3a), which usually strengthens the network to better resist the shrinkage [2,25], nor NaOH concentration (above 0.5 M NaOH) (Fig. 3b) or aging time (Fig. 3c) influence shrinkage, within experimental errors. At 0.1 M NaOH, despite that the amount of NaOH is superior to chitosan cationic groups, shrinkage is heterogeneous not allowing adequate determination of sample volume, see the photo and SEM image in Fig. S2. We suppose that at low NaOH concentrations the chitosan network was not well “stabilized” during coagulation and partially collapsed. We hypothesize that the time needed for complete gel coagulation, which is governed by diffusion and polymer/non-solvent interactions, is an important parameter influencing shrinkage and aerogel properties. Thus the 0.1 M NaOH concentration will not be used in the following. It should be noted that our data follow the trend of shrinkage vs aging time reported in [11]: higher the aging time, lower the shrinkage with no further dependence when aging is longer than 24 h. In the following, aging time is kept at 24 h. Overall, the shrinkage obtained is moderate compared to that

reported for some chitosan aerogels (Table S1) which can be up to 60 % [10,16] and even 90 % [17], or for some other bio-aerogels, between 50 – 95 % [16]. However, because of the numerous parameters involved in the preparation of bio-aerogels (polymer molecular weight, charge and chain flexibility, solvent pH, ionic strength, way of structure formation (via non-solvent induced phase separation or gelation induced by crosslinking), type of non-solvent, way of coagulation, etc.), there is still no clear understanding and control of volume shrinkage, and as a consequence, of aerogel bulk density (see next section).

Figure 3

Cryogels showed no volume shrinkage during freezing and drying, within the experimental errors (Fig. 3a). Lower shrinkage for cryogels as compared to that for aerogels has been reported for cellulose and starch [2,26]. This is an expected result as in the preparation of cryogels there is no step of hydrogel immersion in ethanol and in CO₂, both being non-solvents of native polysaccharides.

3.4. Density, porosity, specific surface area and structure

Bulk density and porosity of aerogels and cryogels are shown in Fig. 4a, b and c as a function of chitosan concentration in the initial solution, NaOH concentration in the coagulation bath and aging time, respectively. The theoretical density, calculated for a hypothetical case of zero shrinkage, is also shown for comparison. Bulk density of aerogels was between 0.07 and 0.26 g/cm³, similar to the values reported in literature (Table S1) [10,11,16,22,27–29]. The density of aerogels is higher than the theoretical density due to the volume shrinkage during solvent exchange and drying. The bulk density of cryogels is lower than that of aerogels when made from

the same chitosan concentration in solution (Fig. 4), it is between 0.03 and 0.12 g/cm³ and is almost equal to the theoretical density thanks to the negligible volume shrinkage (Fig. 3a). As expected, higher is the chitosan concentration, higher is aerogel and cryogel density and lower is the porosity and pore volume (Fig.S4). The density of chitosan xerogel is around 1.30 ±0.15 g/cm³ and thus porosity is very low, around 10 % (Fig. 4a).

Figure 4

The sodium hydroxide concentration does not influence density and porosity of aerogels above 0.5 M NaOH (Fig. 4b). At 4 M NaOH aging time also does not influence the density and the porosity (Fig. 4c), confirming the observations reported in the literature [10].

The specific surface area of chitosan aerogels varies within 200 – 270 m²/g (Fig. 5); it slightly increases with the chitosan concentration (Fig. 5a). The values obtained are similar to those reported in literature (Table S1) [10,11,16,22,27–29]. An increase in NaOH concentration in the coagulation bath slightly increases specific surface area (Fig. 5b).

Figure 5

The surface area of cryogels is much lower, around 50 – 70 m²/g (Fig. 5a). The reason is that pores in cryogels are larger as they constitute the space left by sublimated ice crystals. Nevertheless, the specific surface area of as-prepared chitosan cryogels is higher than that reported in literature (few m²/g) [10,28,30–32], and of cellulose II and starch cryogels, being within 10 – 60 m²/g and below 20 m²/g, respectively [2,26].

The inner morphology of chitosan aerogels and cryogels was studied by SEM, representative examples for each type of material made from chitosan solutions of the same concentration are shown in Fig. 6 at different magnifications. The morphology depends on the drying technique: larger pores were obtained with freeze-drying confirming the lower specific surface area of cryogels as compared to that of aerogels. Similar results have been reported for cellulose II and starch-based aerogels and cryogels [2,26,33]. A SEM image of the xerogel morphology (Figure S1) shows the absence of pores, as expected from its very low porosity.

Figure 6

We roughly estimated the pore size of aerogels and cryogels from SEM images; the results are shown in Fig. S3 of the Supporting Information. In both aerogels and cryogels, the pore size is slightly decreasing with the increase of polymer concentration; the same trend was reported for cellulose aerogels and cryogels [2]. Interestingly, the sizes of the pores in cryogels are rather low, from several hundreds of nanometers to few microns which is much smaller compared to other non-crosslinked chitosan-based materials which underwent freeze-drying (pores of several tens up to few hundreds of microns [34]). The smaller pore size of the chitosan cryogels in the current study compared to many other chitosan freeze-dried materials can be explained as follows. The size of the pores in a freeze-dried material strongly depends on the state of the matter before drying. For example, a polysaccharide solution (agarose [35], hyaluronic acid [36]) can undergo cryogelation during freezing resulting in very large macropores of several tens of microns. Pores and channels from few to several tens of microns were reported for a freeze-dried nanocellulose suspension [37]. Freeze-dried ultrasonicated chitosan-alginate, chitosan-collagen and chitosan-gelatin blends also possess pores of several tens of microns [38]. The evolution of the morphology

of a chitosan network (chitosan solution was dropped in tripolyphosphate solution for different duration, beads post-crosslinked with ethylene glycol diglycidyl ether and freeze-dried) at different stages of coagulation was demonstrated in ref. [39]. Ionic bonds are formed between phosphate groups of tripolyphosphate and amine groups of chitosan. At the early stage of coagulation (called phase inversion in ref. [39]), when the network is not yet formed, large pores and channels of several hundreds of microns were obtained; with the progress of coagulation pores became smaller and channels disappeared. All examples given above demonstrate that in weak gels the morphology of freeze-dried matter is adapting to the shape of growing ice crystals. In our case, the network morphology in the hydrogel is fixed before drying as coagulation is completed, and growing ice crystals are deforming and enlarging the pores but not destroying them. Similar results were obtained for cellulose II and starch hydrogels: the network is formed either during coagulation for cellulose [2], or during retrogradation for starch [26].

Buchtová et al. [2] suggested that an increase of the concentration in a cellulose aerogel decreases the pore size thus increasing the specific surface area supposing that pore wall thickness remains the same. A very minor decrease in the pore size of aerogels can be seen (Fig. S3 of the Supporting Information), which corroborates the slight increase in specific surface area observed in Fig. 5a, but no particular trend can be deduced considering a large dispersion of data and the roughness of the approach.

The average size of pore walls in aerogels and cryogels was also estimated from SEM images: the values are 14.4 ± 3.9 nm and 32 ± 14 nm, respectively, which results in approximately 1 nm and 18 nm after subtracting the thickness (14 nm) of the layer of sputtered platinum. These results were compared with the calculated pore wall thickness D assuming the pore walls are ideal rods of uniform thickness and having the same skeletal density as chitosan:

$$D = 4/(\rho_{bulk} \times S_A) \quad (7)$$

The pore wall thickness for aerogels and cryogels was calculated to be around 1.3 nm and 13 nm, respectively, which fits well with the experimental observation.

The XRD pattern of the initial chitosan powder and of grinded aerogel and cryogel are presented in Fig. 7. The initial powder shows a very broad peak around 10° and a sharper peak centered around 20° , similar to the ones reported for chitins and chitosan of various degrees of acetylation and typical for a semi-crystalline chitosan [40–43]. Aerogels and cryogels show peaks at the same angles but the one at 10° is sharper than that of chitosan powder. This sharp peak is characteristic of a hydrated crystalline chitosan [41]. As cryogels and aerogels present a higher specific surface area than that of the powder, we suppose that these porous materials may adsorb more water vapours than chitosan powder explaining the sharper peak. Aging time and sodium hydroxide concentration do not influence the XRD pattern (data not shown) within the experimental errors.

Figure 7

3.5. Absorption of simulated wound exudate

In view of the potential application of chitosan aerogels and cryogels as wound dressings, the absorption of simulated wound exudate (SWE) was studied as a function of the chitosan concentration. Moisture balance is important to guarantee a good healing process and limit infections [44]. The absorption was monitored during 48 h, which is the duration a dressing is typically used before being replaced [45]. Fig. 8a shows that higher is the concentration of chitosan in the initial solution, and thus lower the porosity (Fig. 4) and pore volume (Fig. S3), lower is the absorption of SWE by both aerogels and cryogels. In all cases, a plateau value is reached within one hour. The absorption values obtained correspond to the higher values of chitosan cryogels and

aerogels reported in the literature [10,11,29–32,34] (Table S1). Because of their high absorption capacity, these materials seem suitable for healing of moist wounds where fluid absorption is necessary to limit bacterial proliferation. In Fig. 8b, the amount of fluid absorbed after one hour shows that higher is the porosity, higher is the absorption, as expected. Cryogels and aerogels of similar porosity show similar values of absorption.

Figure 8

4. CONCLUSIONS

Chitosan cryo- and aerogel monoliths were prepared by non-solvent induced phase separation without crosslinker and characterized. The influence of the process parameters (polymer concentration, non-solvent concentration, time of aging, drying conditions) on the morphology and structural properties of the porous materials was studied. No influence of the aging time was observed within the time frame used. As long as the concentration of the coagulation bath is 0.5 M or higher, it also does not have a major influence on chitosan aerogel or cryogel properties. Chitosan concentration increases density and decreases porosity of both types of materials, as expected.

The main parameter that changes the properties is the method of drying. Supercritical drying allows the preservation of the morphology of the hydrogels resulting in a specific surface area of 200-270 m²/g. Due to the moderate shrinkage of the samples during solvent exchange and drying (within 30 %), the bulk density of aerogels is low, between 0.07 and 0.26 g/cm³. Freeze-drying distorted the morphology of hydrogels due to the growth of ice crystals resulting in larger pores compared to aerogels and in a lower specific surface area. Furthermore, cryogels were of lower density than aerogels and thus of higher porosity. Nevertheless, the pore sizes in cryogels were

surprisingly small (from a few hundreds of nanometers to a few microns) as compared to chitosan materials reported in literature which underwent freeze-drying. It indicates a strong capacity of the network to resist to deformations induced by growing ice crystals during freezing.

In view of the high and tunable SWE absorption, the well-known biocompatibility of chitosan and the small pores which prevent cell ingrowth, these porous chitosan materials are promising materials for wound dressing applications.

Acknowledgements

CNRS is gratefully acknowledged for funding of this project. We thank Pierre Ilbizian (PERSEE, Mines ParisTech, France) for supercritical drying, Gabriel Monge (CEMEF, Mines ParisTech) for performing XRD experiments and Suzanne Jacomet (CEMEF, Mines ParisTech) for help with SEM imaging.

Declarations of interest: none.

References

- [1] S. Groult, S. Buwalda, T. Budtova, Pectin hydrogels, aerogels, cryogels and xerogels: Influence of drying on structural and release properties, *European Polymer Journal*. 149 (2021) 110386. <https://doi.org/10.1016/j.eurpolymj.2021.110386>.
- [2] N. Buchtová, T. Budtova, Cellulose aero-, cryo- and xerogels: towards understanding of morphology control, *Cellulose*. 23 (2016) 2585–2595. <https://doi.org/10.1007/s10570-016-0960-8>.
- [3] A. Anitha, S. Sowmya, P.T.S. Kumar, S. Deepthi, K.P. Chennazhi, H. Ehrlich, M. Tsurkan, R. Jayakumar, Chitin and chitosan in selected biomedical applications, *Progress in Polymer Science*. 39 (2014) 1644–1667. <https://doi.org/10.1016/j.progpolymsci.2014.02.008>.
- [4] M. Dash, F. Chiellini, R.M. Ottenbrite, E. Chiellini, Chitosan—A versatile semi-synthetic polymer in biomedical applications, *Progress in Polymer Science*. 36 (2011) 981–1014. <https://doi.org/10.1016/j.progpolymsci.2011.02.001>.
- [5] T. Jiang, R. James, S.G. Kumbar, C.T. Laurencin, Chitosan as a biomaterial: structure, properties, and applications in tissue engineering and drug delivery, in: *Natural and Synthetic Biomedical Polymers*, Elsevier, 2014: pp. 91–113.
- [6] S. Wei, Y.C. Ching, C.H. Chuah, Synthesis of chitosan aerogels as promising carriers for drug delivery: A review, *Carbohydrate Polymers*. 231 (2020) 115744. <https://doi.org/10.1016/j.carbpol.2019.115744>.
- [7] E.S. Dragan, M.V. Dinu, Advances in porous chitosan-based composite hydrogels: Synthesis and applications, *Reactive and Functional Polymers*. 146 (2020) 104372. <https://doi.org/10.1016/j.reactfunctpolym.2019.104372>.
- [8] J. Radwan-Pragłowska, M. Piątkowski, ł. Janus, D. Bogdał, D. Matysek, Biodegradable, pH-responsive chitosan aerogels for biomedical applications, *RSC Advances*. 7 (2017) 32960–32965. <https://doi.org/10.1039/C6RA27474A>.
- [9] R. Wang, D. Shou, O. Lv, Y. Kong, L. Deng, J. Shen, pH-Controlled drug delivery with hybrid aerogel of chitosan, carboxymethyl cellulose and graphene oxide as the carrier, *International Journal of Biological Macromolecules*. 103 (2017) 248–253. <https://doi.org/10.1016/j.ijbiomac.2017.05.064>.
- [10] C. López-Iglesias, J. Barros, I. Ardao, F.J. Monteiro, C. Alvarez-Lorenzo, J.L. Gómez-Amoza, C.A. García-González, Vancomycin-loaded chitosan aerogel particles for chronic

- wound applications, *Carbohydrate Polymers*. 204 (2019) 223–231. <https://doi.org/10.1016/j.carbpol.2018.10.012>.
- [11] C. López-Iglesias, J. Barros, I. Ardao, P. Gurikov, F.J. Monteiro, I. Smirnova, C. Alvarez-Lorenzo, C.A. García-González, Jet Cutting Technique for the Production of Chitosan Aerogel Microparticles Loaded with Vancomycin, *Polymers*. 12 (2020) 273. <https://doi.org/10.3390/polym12020273>.
- [12] S. Takeshita, S. Yoda, Chitosan Aerogels: Transparent, Flexible Thermal Insulators, *Chemistry of Materials*. 27 (2015) 7569–7572. <https://doi.org/10.1021/acs.chemmater.5b03610>.
- [13] S. Takeshita, S. Zhao, W.J. Malfait, Transparent, Aldehyde-Free Chitosan Aerogel, *Carbohydrate Polymers*. 251 (2021) 117089. <https://doi.org/10.1016/j.carbpol.2020.117089>.
- [14] S. Takeshita, S. Zhao, W.J. Malfait, M.M. Koebel, *Chemistry of Chitosan Aerogels: Three-Dimensional Pore Control for Tailored Applications*, *Angewandte Chemie International Edition*. (2020). <https://doi.org/10.1002/anie.202003053>.
- [15] R.M. Obaidat, B.M. Tashtoush, M.F. Bayan, R. T. Al Bustami, M. Alnaief, Drying Using Supercritical Fluid Technology as a Potential Method for Preparation of Chitosan Aerogel Microparticles, *AAPS PharmSciTech*. 16 (2015) 1235–1244. <https://doi.org/10.1208/s12249-015-0312-2>.
- [16] F. Quignard, R. Valentin, F. Di Renzo, Aerogel materials from marine polysaccharides, *New Journal of Chemistry*. 32 (2008) 1300. <https://doi.org/10.1039/b808218a>.
- [17] S. Takeshita, A. Sadeghpour, W.J. Malfait, A. Konishi, K. Otake, S. Yoda, Formation of Nanofibrous Structure in Biopolymer Aerogel during Supercritical CO₂ Processing: The Case of Chitosan Aerogel, *Biomacromolecules*. 20 (2019) 2051–2057. <https://doi.org/10.1021/acs.biomac.9b00246>.
- [18] G.K. Moore, G.A.F. Roberts, Determination of the degree of N-acetylation of chitosan, (n.d) 2.
- [19] S. Groult, T. Budtova, Thermal conductivity/structure correlations in thermal super-insulating pectin aerogels, *Carbohydrate Polymers*. 196 (2018) 73–81. <https://doi.org/10.1016/j.carbpol.2018.05.026>.

- [20] L. Druel, R. Bardl, W. Vorweg, T. Budtova, Starch Aerogels: A Member of the Family of Thermal Superinsulating Materials, *Biomacromolecules*. 18 (2017) 4232–4239. <https://doi.org/10.1021/acs.biomac.7b01272>.
- [21] G.A. Roberts, J.G. Domszy, Determination of the viscometric constants for chitosan, *International Journal of Biological Macromolecules*. 4 (1982) 374–377.
- [22] A. Tabernero, L. Baldino, A. Misol, S. Cardea, E.M.M. del Valle, Role of rheological properties on physical chitosan aerogels obtained by supercritical drying, *Carbohydrate Polymers*. 233 (2020) 115850. <https://doi.org/10.1016/j.carbpol.2020.115850>.
- [23] M. Robitzer, F.D. Renzo, F. Quignard, Natural materials with high surface area. Physisorption methods for the characterization of the texture and surface of polysaccharide aerogels, *Microporous and Mesoporous Materials*. 140 (2011) 9–16. <https://doi.org/10.1016/j.micromeso.2010.10.006>.
- [24] T. Tanaka, Collapse of Gels and the Critical Endpoint, *Phys. Rev. Lett.* 40 (1978) 820–823. <https://doi.org/10.1103/PhysRevLett.40.820>.
- [25] S. Groult, T. Budtova, Tuning structure and properties of pectin aerogels, *European Polymer Journal*. 108 (2018) 250–261. <https://doi.org/10.1016/j.eurpolymj.2018.08.048>.
- [26] F. Zou, T. Budtova, Tailoring the morphology and properties of starch aerogels and cryogels via starch source and process parameter, *Carbohydrate Polymers*. 255 (2021) 117344. <https://doi.org/10.1016/j.carbpol.2020.117344>.
- [27] F. Di Renzo, R. Valentin, M. Boissière, A. Tourrette, G. Sparapano, K. Molvinger, J.-M. Devoisselle, C. Gérardin, F. Quignard, Hierarchical Macroporosity Induced by Constrained Syneresis in Core–Shell Polysaccharide Composites, *Chemistry of Materials*. 17 (2005) 4693–4699. <https://doi.org/10.1021/cm0503477>.
- [28] M. Díez-Municio, A. Montilla, M. Herrero, A. Olano, E. Ibáñez, Supercritical CO₂ impregnation of lactulose on chitosan: A comparison between scaffolds and microspheres form, *The Journal of Supercritical Fluids*. 57 (2011) 73–79. <https://doi.org/10.1016/j.supflu.2011.02.001>.
- [29] D. Lovskaya, N. Menshutina, M. Mochalova, A. Nosov, A. Grebenyuk, Chitosan-Based Aerogel Particles as Highly Effective Local Hemostatic Agents. Production Process and In Vivo Evaluations, *Polymers*. 12 (2020) 2055. <https://doi.org/10.3390/polym12092055>.

- [30] Y.-C. Wang, M.-C. Lin, D.-M. Wang, H.-J. Hsieh, Fabrication of a novel porous PGA-chitosan hybrid matrix for tissue engineering, *Biomaterials*. 24 (2003) 1047–1057.
- [31] T.-W. Sun, W.-L. Yu, Y.-J. Zhu, F. Chen, Y.-G. Zhang, Y.-Y. Jiang, Y.-H. He, Porous Nanocomposite Comprising Ultralong Hydroxyapatite Nanowires Decorated with Zinc-Containing Nanoparticles and Chitosan: Synthesis and Application in Bone Defect Repair, *Chemistry - A European Journal*. 24 (2018) 8809–8821. <https://doi.org/10.1002/chem.201800425>.
- [32] H.B. Tan, F.Y. Wang, W. Ding, Y. Zhang, J. Ding, D.X. Cai, K.F. Yu, J. Yang, L. Yang, Y.Q. Xu, Fabrication and evaluation of porous keratin/chitosan (KCS) scaffolds for effectively accelerating wound healing, *Biomed Environ Sci*. 28 (2015) 178–89.
- [33] N. Buchtová, C. Pradille, J.-L. Bouvard, T. Budtova, Mechanical properties of cellulose aerogels and cryogels, *Soft Matter*. 15 (2019) 7901–7908. <https://doi.org/10.1039/C9SM01028A>.
- [34] Y. Fan, Q. Lu, W. Liang, Y. Wang, Y. Zhou, M. Lang, Preparation and characterization of antibacterial polyvinyl alcohol/chitosan sponge and potential applied for wound dressing, *European Polymer Journal*. 157 (2021) 110619. <https://doi.org/10.1016/j.eurpolymj.2021.110619>.
- [35] V.I. Lozinsky, L.G. Damshkaln, K.O. Bloch, P. Vardi, N.V. Grinberg, T.V. Burova, V.Y. Grinberg, Cryostructuring of polymer systems. XXIX. Preparation and characterization of supermacroporous (spongy) agarose-based cryogels used as three-dimensional scaffolds for culturing insulin-producing cell aggregates, *J. Appl. Polym. Sci*. 108 (2008) 3046–3062. <https://doi.org/10.1002/app.27908>.
- [36] Z. Cai, F. Zhang, Y. Wei, H. Zhang, Freeze–Thaw-Induced Gelation of Hyaluronan: Physical Cryostructuring Correlated with Intermolecular Associations and Molecular Conformation, *Macromolecules*. 50 (2017) 6647–6658. <https://doi.org/10.1021/acs.macromol.7b01264>.
- [37] F. Martoia, T. Cochereau, P.J.J. Dumont, L. Orgéas, M. Terrien, M.N. Belgacem, Cellulose nanofibril foams: Links between ice-templating conditions, microstructures and mechanical properties, *Materials & Design*. 104 (2016) 376–391. <https://doi.org/10.1016/j.matdes.2016.04.088>.
- [38] N. Naghshineh, K. Tahvildari, M. Nozari, Preparation of Chitosan, Sodium Alginate, Gelatin and Collagen Biodegradable Sponge Composites and their Application in Wound Healing

- and Curcumin Delivery, *Journal of Polymers and the Environment*. 27 (2019) 2819–2830. <https://doi.org/10.1007/s10924-019-01559-z>.
- [39] F. Mi, Adsorption of indomethacin onto chemically modified chitosan beads, *Polymer*. 43 (2002) 757–765. [https://doi.org/10.1016/S0032-3861\(01\)00580-8](https://doi.org/10.1016/S0032-3861(01)00580-8).
- [40] Y.-W. Cho, J. Jang, C.R. Park, S.-W. Ko, Preparation and Solubility in Acid and Water of Partially Deacetylated Chitins, *Biomacromolecules*. 1 (2000) 609–614. <https://doi.org/10.1021/bm000036j>.
- [41] R. Barreiro-Iglesias, R. Coronilla, A. Concheiro, C. Alvarez-Lorenzo, Preparation of chitosan beads by simultaneous cross-linking/insolubilisation in basic pH, *European Journal of Pharmaceutical Sciences*. 24 (2005) 77–84. <https://doi.org/10.1016/j.ejps.2004.09.013>.
- [42] K. Harish Prashanth, Solid state structure of chitosan prepared under different N-deacetylating conditions, *Carbohydrate Polymers*. 50 (2002) 27–33. [https://doi.org/10.1016/S0144-8617\(01\)00371-X](https://doi.org/10.1016/S0144-8617(01)00371-X).
- [43] M.-T. Yen, J.-H. Yang, J.-L. Mau, Physicochemical characterization of chitin and chitosan from crab shells, *Carbohydrate Polymers*. 75 (2009) 15–21. <https://doi.org/10.1016/j.carbpol.2008.06.006>.
- [44] T.D. Turner, Hospital usage of absorbent dressings, *Pharmaceutical Journal*. 222 (1979) 421–424.
- [45] C. Lindholm, T.J. Styche, H.E. Horton, Diagnosis and treatment impacts on wound care efficiency drivers: real-world analysis, *J Wound Care*. 30 (2021) 534–542. <https://doi.org/10.12968/jowc.2021.30.7.534>.

Legends

Figure 1. Schematic representation of the preparation of chitosan aerogels and cryogels.

Figure 2. Photos of chitosan aerogels and cryogels. Top line: aerogels made from solutions of chitosan of various concentrations (1 % wt/v, 3 % wt/v, 5 % wt/v and 7 % wt/v), coagulated in 4 M NaOH and aged for 24 h; middle line: aerogels from solutions of 5 % wt/v chitosan coagulated in 0.1 M, 1 M and 4 M NaOH and aged for 24 h, and bottom line: cryogels from solutions of chitosan of various concentrations (5 % wt/v, 6 % wt/v, 7 % wt/v and 8 % wt/v) coagulated in 4 M NaOH and aged for 24 h.

Figure 3. Volume shrinkage during the preparation of chitosan aerogels, cryogels and xerogel as a function of (a) the chitosan concentration in solution (all samples coagulated in 4 M NaOH and aged for 24 h), (b) NaOH concentration in coagulation bath (chitosan solution was 5 % wt/v, all samples aged during 24 h) and (c) aging time (chitosan solution was 5 % wt/v, all samples coagulated in 4 M NaOH). Lines are given to guide the eye.

Figure 4. Bulk density (in black) and porosity (in blue) of chitosan aerogels (filled circles), cryogels (filled triangles) and xerogel (filled square) as a function of the (a) chitosan concentration in solution (coagulation in 4 M NaOH, 24 h aging), (b) NaOH concentration in the coagulation bath (5 % wt/v chitosan solution, 24 h aging) and (c) aging time (5 % wt/v chitosan solution, 4 M NaOH). Solid lines correspond to theoretical density in case of no shrinkage. Dashed lines are given to guide the eye. If error bars are not seen, they are smaller than the symbol.

Figure 5. Specific surface area of aerogels (filled circles) and cryogels (filled triangles) as a function of (a) chitosan concentration in solution (coagulation in 4 M NaOH, 24 h aging) and (b) NaOH concentration (5 % wt/v chitosan solution, 24 h aging).

Figure 6. SEM images of chitosan aerogels (top line) and cryogels (bottom line). The chitosan concentration was 5 % wt/v (left column) and 7 % wt/v (right column). Samples were coagulated in 4 M NaOH and aged for 24 h.

Figure 7. XRD diffraction patterns of the initial chitosan powder, cryogel and aerogel. The cryogel and aerogel were made from 5 % wt/v dissolved chitosan, coagulated in 4 M NaOH and aged for 24 h.

Figure 8. (a) Absorption kinetics of SWE at 30 °C for cryogels and aerogels made from 3, 4, 5, 6, 7, 8 and 10 % wt/v of chitosan solutions (aged for 24 h in 4 M NaOH), (b) SWE sorption after 1 h as a function of material porosity: blue triangles are for cryogels and red circles are for aerogels.

Tuning the properties of porous chitosan: aerogels and cryogels

Coraline Chartier, Sytze Buwalda, H el ene Van Den Berghe, Benjamin Nottelet, Tatiana Budtova

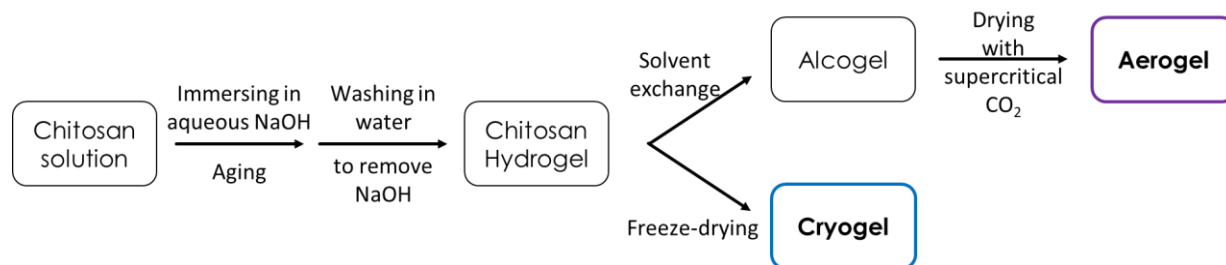


Figure 1

Tuning the properties of porous chitosan: aerogels and cryogels

Coraline Chartier, Sytze Buwalda, H el ene Van Den Berghe, Benjamin Nottelet, Tatiana Budtova



Figure 2

Tuning the properties of porous chitosan: aerogels and cryogels

Coraline Chartier, Sytze Buwalda, Hélène Van Den Berghe, Benjamin Nottelet, Tatiana Budtova

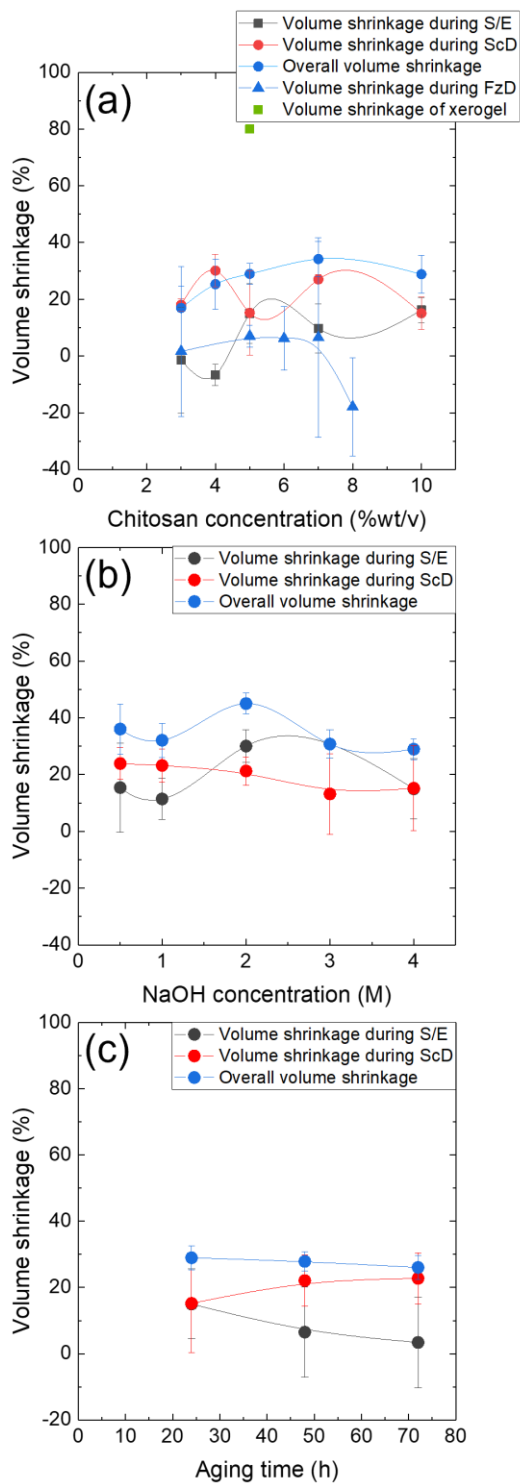


Figure 3

Tuning the properties of porous chitosan: aerogels and cryogels

Coraline Chartier, Sytze Buwalda, Hélène Van Den Berghe, Benjamin Nottelet, Tatiana Budtova

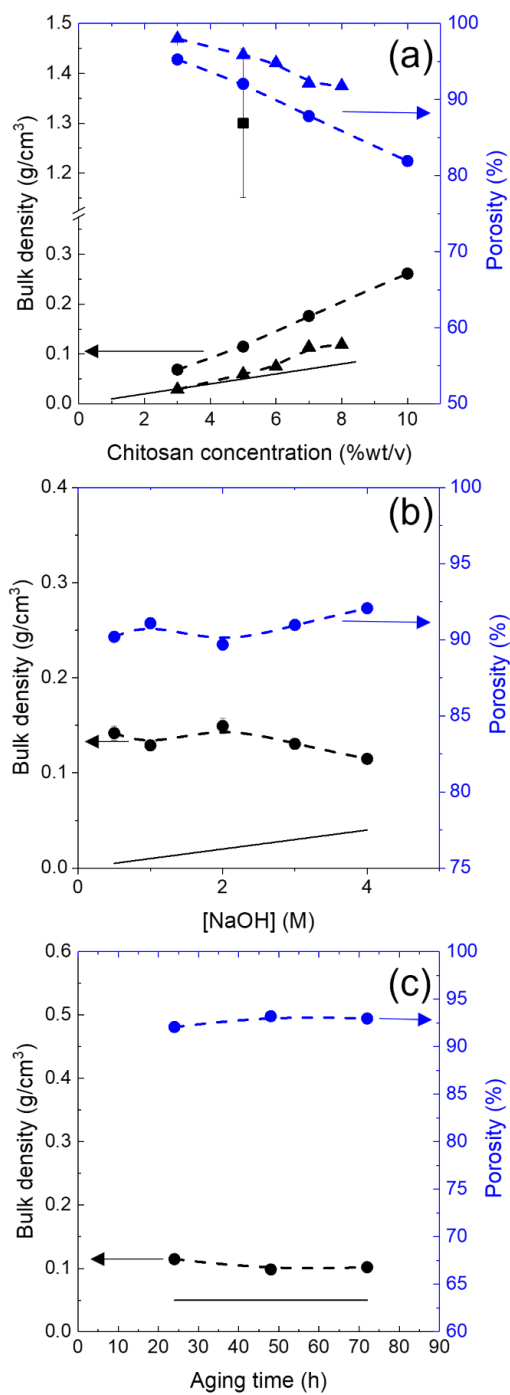


Figure 4

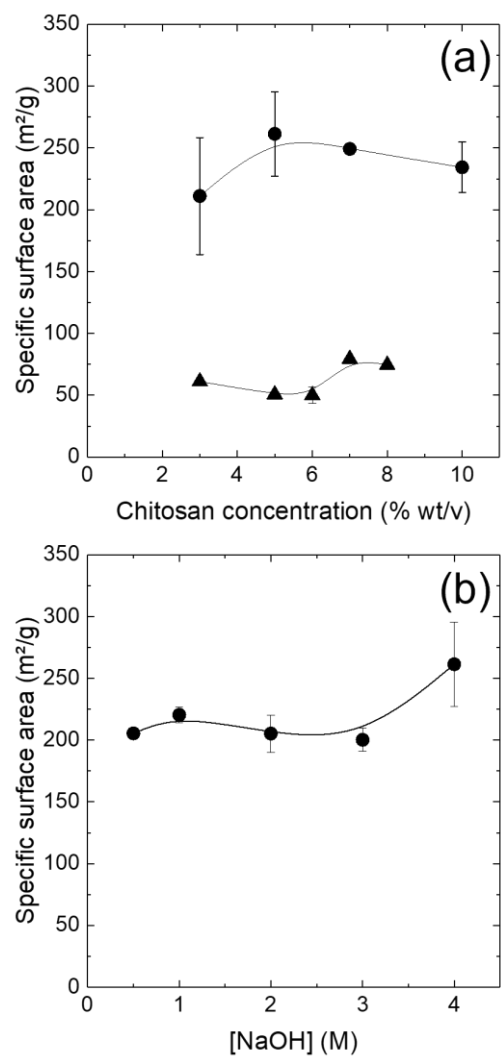


Figure 5

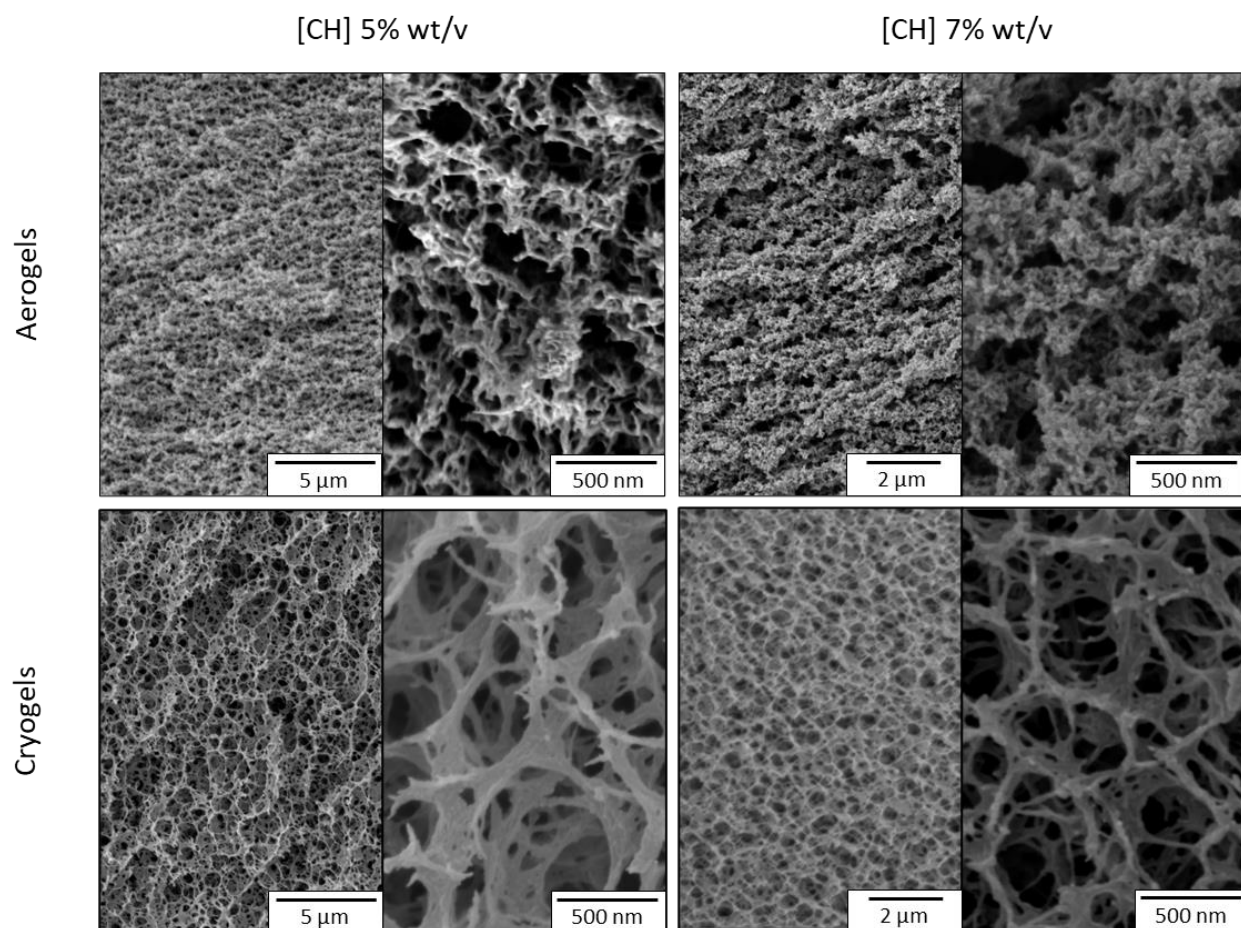


Figure 6

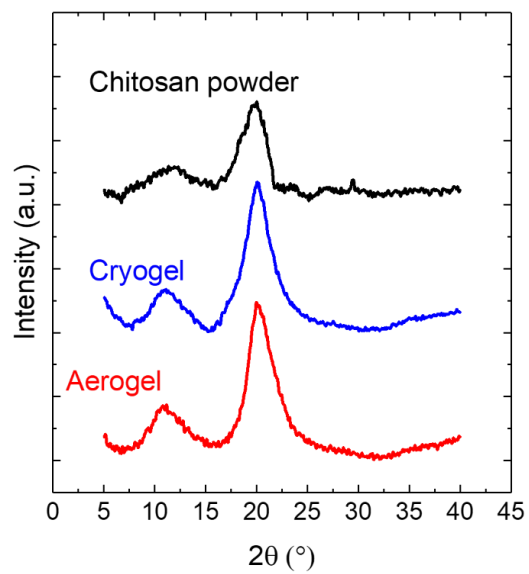


Figure 7

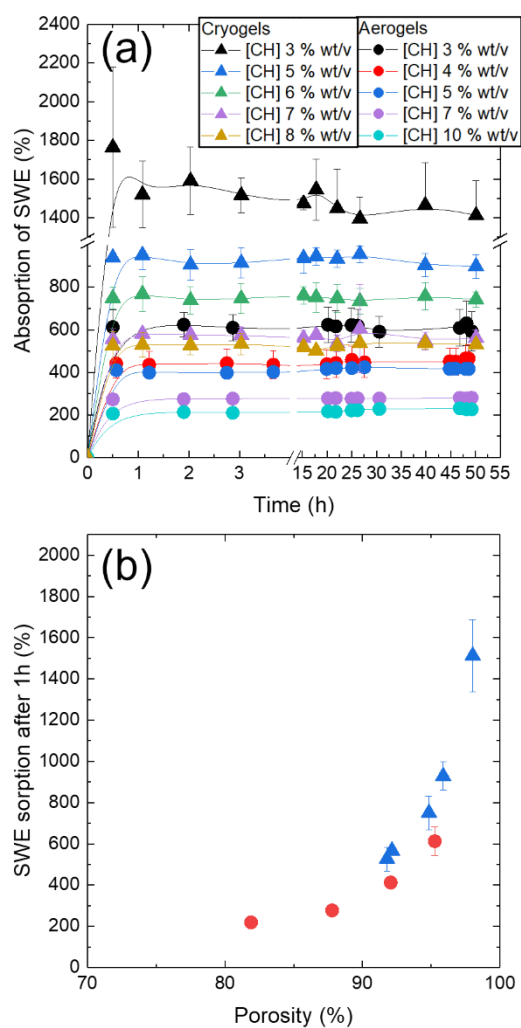


Figure 8

Supporting information

Tuning the properties of porous chitosan: aerogels and cryogels

Coraline Chartier,^a Sytze Buwalda,^a H el ene Van Den Berghe,^b Benjamin Nottelet,^b

Tatiana Budtova^{a}*

^aMINES ParisTech, PSL Research University, Center for Materials Forming (CEMEF), UMR
CNRS 7635, CS 10207, 06904 Sophia Antipolis, France

^bDepartment of Polymers for Health and Biomaterials, IBMM, Univ Montpellier, CNRS,
ENSCM, Montpellier, France

*Corresponding author.

Tatiana Budtova, tatiana.budtova@minesparis.psl.eu

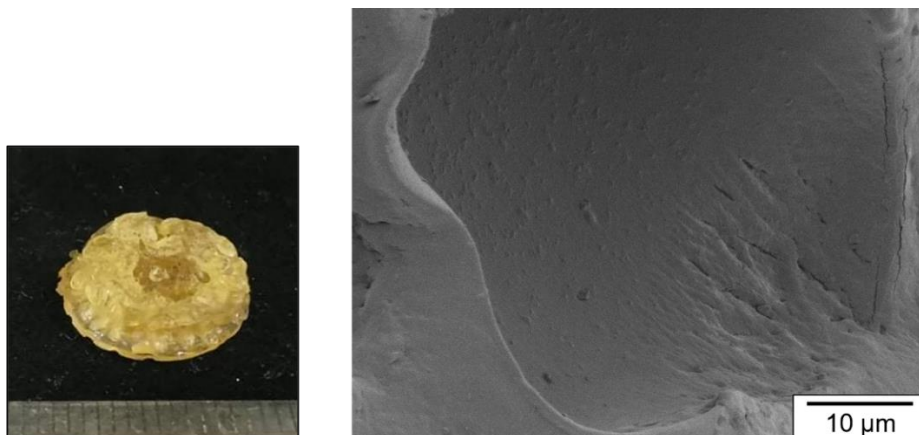


Figure S1

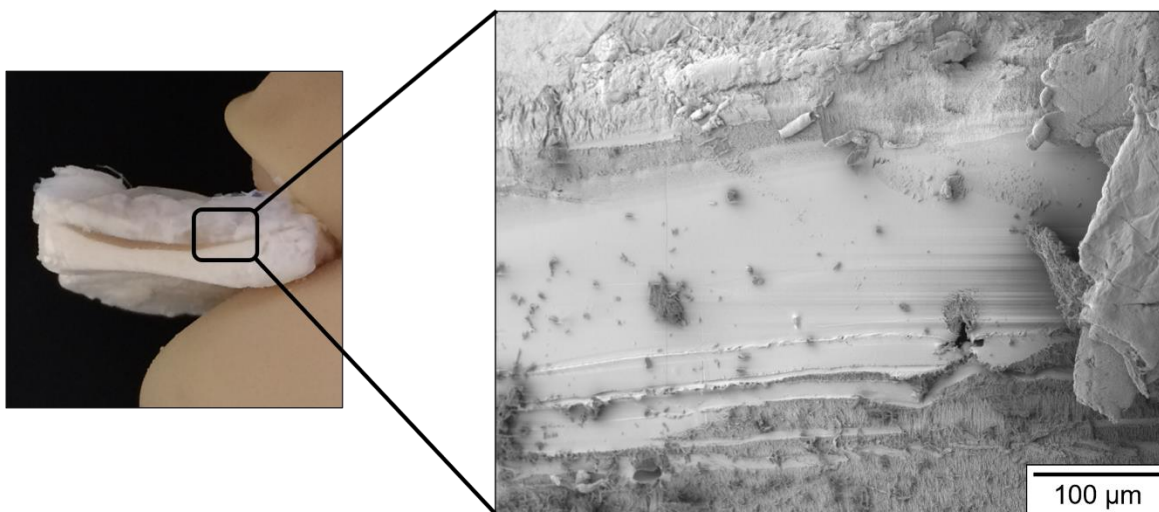
Photo and SEM image of chitosan xerogel made from 5% wt/v chitosan solution, coagulated in 4 M of NaOH solution and aged for 24 h.

Table S1: Characteristics of aerogels and cryogels made from non-crosslinked chitosan as a function of processing parameters, taken from literature. Density values marked with “*” were calculated from the data reported for porosity, with $\rho_s = 1.446 \text{ g/cm}^3$ [1]. FzD: freeze-drying, ScD: supercritical drying.

Chitosan concentration (%wt/v)	DA	Molecular weight (kDa)	Acetic acid concentration	Aging time (h)	NaOH concentration (M)	Drying method	Volume shrinkage (%)	Bulk density (g/cm ³)	Porosity (%)	Specific surface area (m ² /g)	Absorption (%)	Reference
2.5	10	200 - 400	1%	0.5	0.1	ScD	55.8	0.046	96.8	360	N.A.	[1]
2.5	10	200 - 400	1%	1	0.1	ScD	53.3	0.046	96.8	343	380% of PBS in 24 h	[1]
2.5	10	200 - 400	1%	2	0.1	ScD	52.6	0.049	96.6	386	N.A.	[1]
2.5	10	200 - 400	1%	4	0.1	ScD	41.3	0.041	97.2	479	N.A.	[1]
2.5	10	200 - 400	1%	10	0.1	ScD	38.3	0.041	97.2	257	N.A.	[1]
2.5	10	200 - 400	1%	24	0.1	ScD	35.0	0.042	97.1	324	N.A.	[1]
2.5	10	200 - 400	1%	N.A.	0.1	FzD	95.9	0.535	63.0	N.A.	N.A.	[1]
2	10	200 - 400	1%	1	0.2	ScD	N.A.	N.A.	N.A.	N.A.	900% of PBS in 24 h	[2]
2.5	5	200	0.055 M	N.A.	4	ScD	60	N.A.	N.A.	330	N.A.	[3]
1	10	500	0.055 M	N.A.	4	ScD	N.A.	0.0289*	98	175	N.A.	[4]
1	15	350	2%	N.A.	1.25	ScD	N.A.	0.1605*	88.9	111	N.A.	[5]
1	15	350	2%	N.A.	1.25	FzD	N.A.	0.0216*	98.3	3.6	N.A.	[5]
1	N.A.	111	0.1 M	12	4	ScD	N.A.	0.0488	97.94	301	963% of water in 30 min	[6]

1	N.A.	125	0.1 M	12	4	ScD	N.A.	0.0569	96.77	262	740% of water in 30 min	[6]
1	N.A.	294	0.1 M	12	4	ScD	N.A.	0.0761	95.89	254	589% of water in 30 min	[6]
1	N.A.	343	0.1 M	12	4	ScD	N.A.	0.0802	96.16	243	483% of water in 30 min	[6]
1	N.A.	250	3%	N.A.	1	ScD	N.A.	0.090	94	115	N.A.	[7]
2	N.A.	250	3%	N.A.	1	ScD	N.A.	0.112	92	125	N.A.	[7]
3	N.A.	250	3%	N.A.	1	ScD	N.A.	0.137	90	110	N.A.	[7]
3	N.A.	N.A.	1%	12	1	FzD	N.A.	0.1414*	90.22	N.A.	1365% of water in 24 h	[8]
3	6	440	0.2M	0.5	1	FzD	N.A.	0.3326	77	N.A.	310% of PBS in 13 h	[9]
N.A.	10	100	N.A	N.A.	N.A.	FzD	N.A.	0.1446	90	N.A.	250% of PBS in 2h	[10]
2	10	50	1%	N.A.	N.A.	FzD	N.A.	0.2169*	85	N.A.	900% of water in 24 h	[11]

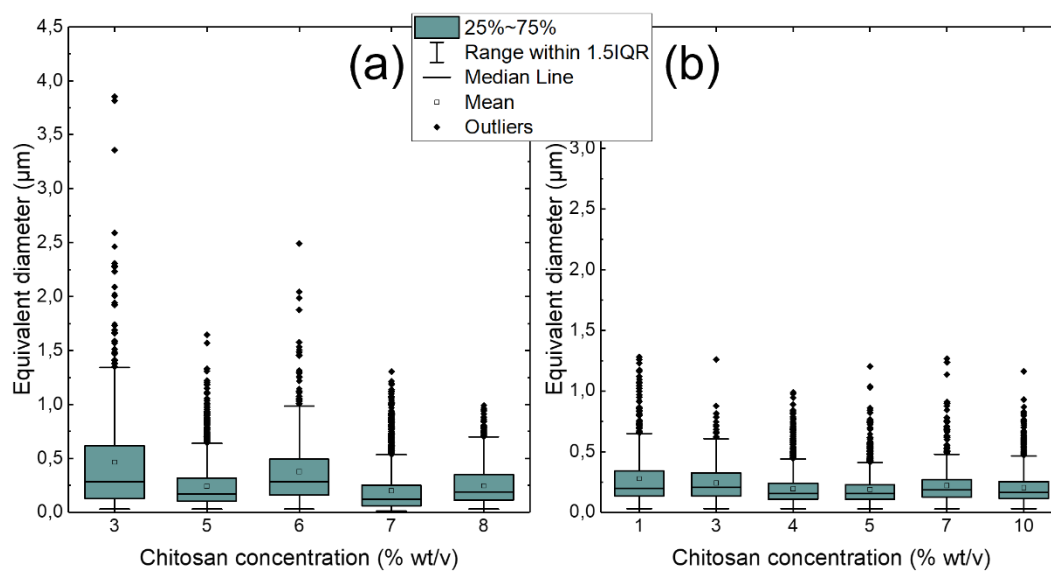
1
2



3
4
5
6
7

Figure S2

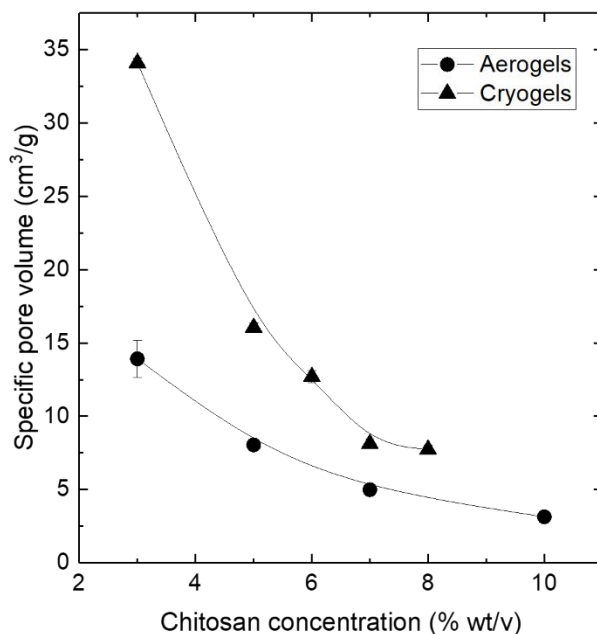
Photo and SEM image of chitosan aerogel sample made from 5% wt/v of chitosan solution, coagulated in 0.1M of NaOH and aged for 24 h.



8
9

Figure S3

1 Box plot of the pore size distribution in chitosan cryogels (a) and aerogels (b) (values obtained
2 from the analysis of SEM images at 10000x magnification).



3
4 Figure S4
5 Specific pore volume in chitosan aerogels (circles) and cryogels (triangles). Lines are given to
6 guide the eye.

8 References

- 9 [1] C. López-Iglesias, J. Barros, I. Ardao, F.J. Monteiro, C. Alvarez-Lorenzo, J.L. Gómez-Amoza, C.A. García-
10 González, Vancomycin-loaded chitosan aerogel particles for chronic wound applications, *Carbohydrate Polymers*. 204 (2019) 223–231. <https://doi.org/10.1016/j.carbpol.2018.10.012>.
11
12 [2] C. López-Iglesias, J. Barros, I. Ardao, P. Gurikov, F.J. Monteiro, I. Smirnova, C. Alvarez-Lorenzo, C.A.
13 García-González, Jet Cutting Technique for the Production of Chitosan Aerogel Microparticles Loaded
14 with Vancomycin, *Polymers*. 12 (2020) 273. <https://doi.org/10.3390/polym12020273>.
15 [3] F. Quignard, R. Valentin, F. Di Renzo, Aerogel materials from marine polysaccharides, *New Journal of*
16 *Chemistry*. 32 (2008) 1300. <https://doi.org/10.1039/b808218a>.

- 1 [4] F. Di Renzo, R. Valentin, M. Boissière, A. Tournette, G. Sparapano, K. Molvinger, J.-M. Devoisselle, C.
2 Gérardin, F. Quignard, Hierarchical Macroporosity Induced by Constrained Syneresis in Core–Shell
3 Polysaccharide Composites, *Chemistry of Materials*. 17 (2005) 4693–4699.
4 <https://doi.org/10.1021/cm0503477>.
- 5 [5] M. Díez-Municio, A. Montilla, M. Herrero, A. Olano, E. Ibáñez, Supercritical CO₂ impregnation of
6 lactulose on chitosan: A comparison between scaffolds and microspheres form, *The Journal of*
7 *Supercritical Fluids*. 57 (2011) 73–79. <https://doi.org/10.1016/j.supflu.2011.02.001>.
- 8 [6] D. Lovskaya, N. Menshutina, M. Mochalova, A. Nosov, A. Grebenyuk, Chitosan-Based Aerogel
9 Particles as Highly Effective Local Hemostatic Agents. Production Process and In Vivo Evaluations,
10 *Polymers*. 12 (2020) 2055. <https://doi.org/10.3390/polym12092055>.
- 11 [7] A. Tabernerero, L. Baldino, A. Misol, S. Cardea, E.M.M. del Valle, Role of rheological properties on
12 physical chitosan aerogels obtained by supercritical drying, *Carbohydrate Polymers*. 233 (2020)
13 115850. <https://doi.org/10.1016/j.carbpol.2020.115850>.
- 14 [8] W. Sun, G. Chen, F. Wang, Y. Qin, Z. Wang, J. Nie, G. Ma, Polyelectrolyte-complex multilayer
15 membrane with gradient porous structure based on natural polymers for wound care, *Carbohydrate*
16 *Polymers*. 181 (2018) 183–190. <https://doi.org/10.1016/j.carbpol.2017.10.068>.
- 17 [9] Y.-C. Wang, M.-C. Lin, D.-M. Wang, H.-J. Hsieh, Fabrication of a novel porous PGA-chitosan hybrid
18 matrix for tissue engineering, *Biomaterials*. 24 (2003) 1047–1057.
- 19 [10] H.B. Tan, F.Y. Wang, W. Ding, Y. Zhang, J. Ding, D.X. Cai, K.F. Yu, J. Yang, L. Yang, Y.Q. Xu, Fabrication
20 and evaluation of porous keratin/chitosan (KCS) scaffolds for effectively accelerating wound healing,
21 *Biomed Environ Sci*. 28 (2015) 178–89.
- 22 [11] Y. Fan, Q. Lu, W. Liang, Y. Wang, Y. Zhou, M. Lang, Preparation and characterization of antibacterial
23 polyvinyl alcohol/chitosan sponge and potential applied for wound dressing, *European Polymer*
24 *Journal*. 157 (2021) 110619. <https://doi.org/10.1016/j.eurpolymj.2021.110619>.

25
26